Fabrication and Characterization of The Fizeau Interferometer Testbed

Peter Petrone III[a], Ken Carpenter[b], Dave Clark[b], Paul Cottle[a], Peter Dogoda[a],
Hubert Huet[a], Peter Liiva[a], Richard G. Lyon[b], Joe Marzouk[a], Lisa M. Mazzuca[b]
Dave McAndrew[c], Gregory Solyar[d]

[a]Sigma Space Corporation, Landham, MD. 20706
[b]NASA GSFC, Greenbelt, MD. 20771
[c]Mink Hollow Systems, Highland, MD. 20777
[d]GEST/UMBC, NASA GSFC, Greenbelt, MD. 20771

Abstract

The Fizeau Interferometer Testbed (FIT) is a ground-based system that will be used for the development and testing of technologies relevant to Stellar Imager (SI) and other sparse aperture/Fizeau imaging interferometer mission concepts. The testbed will utilize image-based wavefront sensing and control to co-phase and maintain closed-loop control over a Sparse Aperture Array (SAA) consisting of spherical mirror elements. The SAA is a re-configurable assembly baselined to incorporate between seven (initially) and thirty 12.5mm diameter (R = 4000mm) mirror elements. In this paper we describe the fabrication, alignment, and initial calibration of the phase I (7 primary elements) FIT hardware and discuss various factors impacting the performance and stability of the testbed.

1. Introduction

Stellar Imager (SI) is conceived as a space-based UV/optical interferometry mission designed to study stellar magnetic activity and internal structure. SI will have an angular resolution on the order of 0.1 milli-arcseconds allowing it to image the surface of stars, and reveal information on stellar internal structure and transport mechanisms using asteroseismology. SI will study variations in the magnetic activity of stars (both spatial and temporal) in order to provide improved forecasting of stellar magnetic activity and its impact on planetary climates. The observatory will employ twenty (20) or more one-meter class spherical mirror elements distributed in a reconfigurable pattern over a baseline of approximately 0.5 km. The individual mirror elements will be positioned to form a sparsely populated spherical "virtual" primary mirror so that light beams from all segments can be combined simultaneously at the instrument focal plane [1].

The Fizeau Interferometer Testbed (FIT) is a ground-based system supporting the development and validation of technologies relevant to Stellar Imager and other space-based interferometry missions. FIT will be used to define of a set of baseline requirements for Stellar Imager by identifying and quantifying a variety of factors influencing system wavefront accuracy and stability. The ultimate goal of the testbed is to dynamically monitor and correct system wavefront through the closed-loop control of the seven FIT mirror elements [4,6].

FIT will help develop the system level requirements for future flight missions by investigating the influence of mechanical/thermal stability, vibration, and stray light control on the various phase retrieval and phase diversity approaches under consideration for SI. In addition to studying these environmental effects, the testbed will be used to evaluate various options for sampling the Fourier u-v plane. Such testing will provide guidance on the optimization of future flight configurations by studying the trades involving the number of deployed segments, segment size and deployed formations.

The FIT Primary Mirror Array (PMA) plate employs (7) spherical mirror segments (f = 2000mm) configured in a minimum-redundancy pattern [2,3]. Each mirror segment has five degrees of freedom (tip, tilt, piston and X-Y

decenter). Segment tip/tilt and piston motions are computer controlled however, X-Y decenters currently require manually repositioning the mirror elements on the PMA (grid with 1" centers).

2. System Design Overview

2.1 Optical System Design

The main components of the FIT optical system are the Source Module (SM), collimating/imaging optics and the primary mirror array plate (figure #1).

PRIMARY MIRROR ARRAY
X = 0 mm
Y = +2400 mm

SOURCE
X = +200 mm
Y = +381 mm

COLLIMATING PRIMARY
X = 0 mm
Y = 0 mm

COLLIMATING SECONDARY
X = +146 mm
Y = +2195 mm

Y

FOLD MIRROR
X = -235 mm
Y = +2280 mm

IMAGING SECONDARY
X = -200 mm
Y = +980 mm

IMAGE PLANE
X = -395 mm
Y = +640 mm

NOMINAL Z-AXIS
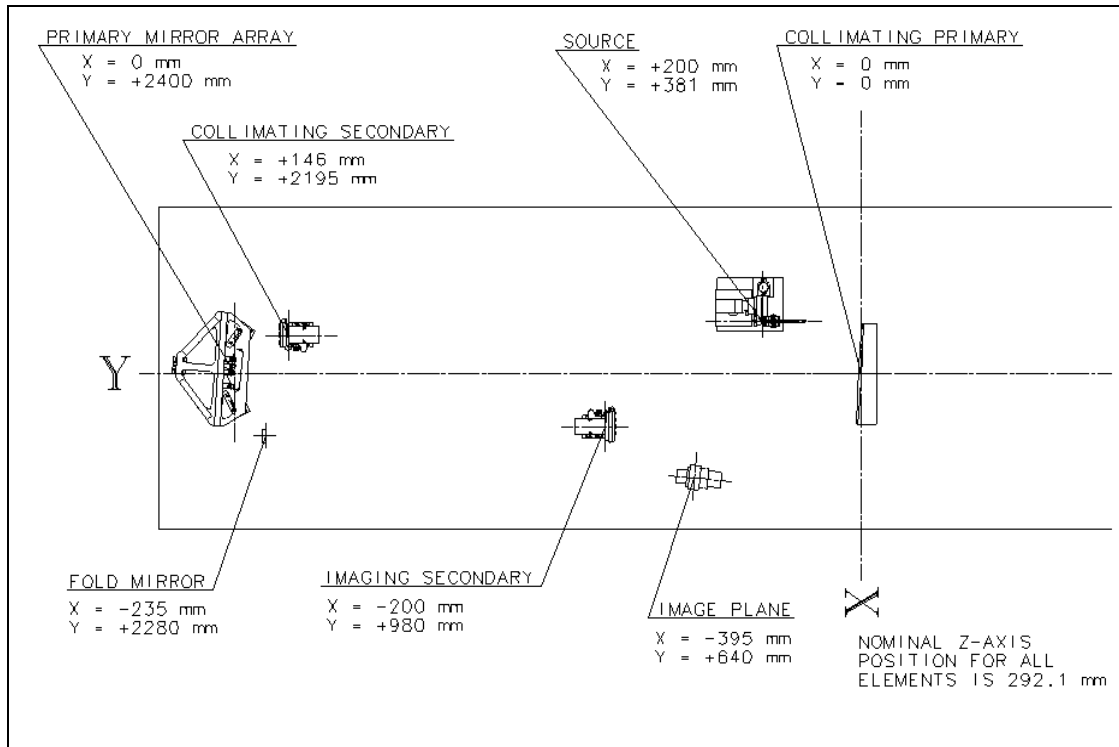POSITION FOR ALL
ELEMENTS IS 292.1 mm

Figure #1

An extended scene or point source (pinhole) is introduced to the system by placing it at the focal plane of the collimating optics; which consist of a custom 4" hyperboloid manufactured by Torus Technologies and a commercial 12 inch Off Axis Parabola (OAP) supplied by Ealing Optical [9]. Collimated light from the OAP is delivered to the FIT PMA and is then relayed to the imaging secondary mirror, a 5" oblate ellipsoid also manufactured by Torus Technologies. Light reflected from the imaging secondary is delivered to a fold flat before coming to focus at the image plane of the CCD. A Pellicle beamsplitter intercepts the converging beam leaving the final fold so that both the reflected and transmitted light may be simultaneously recorded using two identical CCD cameras.

Automated linear stages controlled by a National Instruments ESP-300 driver box are used for scene selection and for setting camera(s) focus positions. Additionally, each of the seven mirror elements comprising the Primary Mirror Array (PMA) uses a computer controlled PZT stage for adjusting tip/tilt and piston.

 Future modifications include replacing the two-camera setup with an optical trombone and a single CCD camera. The optical trombone splits the input beam into two paths (having a differential OPD) and delivers both beams to a single CD camera for simultaneous capture. Figure #2 shows the functional relationship between the various FIT components.
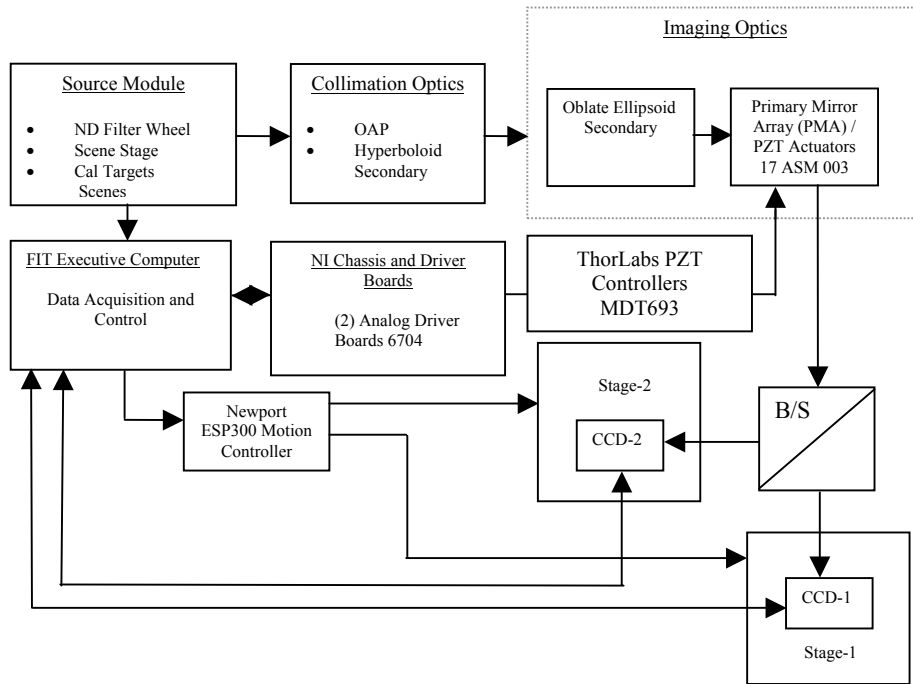
FIT Functional Diagram

Imaging Optics

| Source Module | Collimation Optics | Oblate Ellipsoid Secondary | Primary Mirror Array (PMA) / PZT Actuators 17 ASM 003 |

Source Module
- ND Filter Wheel
- Scene Stage
- Cal Targets Scenes

Collimation Optics
- OAP
- Hyperboloid Secondary

Oblate Ellipsoid Secondary

Primary Mirror Array (PMA) / PZT Actuators 17 ASM 003

FIT Executive Computer

Data Acquisition and Control

NI Chassis and Driver Boards

(2) Analog Driver Boards 6704

ThorLabs PZT Controllers MDT693

Newport ESP300 Motion Controller

Stage-2

CCD-2

B/S

CCD-1

Stage-1

Figure #2

2.2 Mechanical System Design Considerations

The FIT optics are mounted on a 16' X 4' Kinetic Systems Inc. series 500 vibration isolated optical table.
Since FIT is essentially an interferometer, long-term stability was the dominant mechanical design requirement. System instabilities may manifest themselves as line of sight (LOS) motions, jitter and differential motions associated with the segments on the primary mirror array. From an operational and performance standpoint, differential motions (segment to segment) are the least desirable, since they have the potential to de-phase the PMA.

In keeping with cost and time constraints, most of the system was constructed using off the shelf components. The mounts for the PMA, collimating secondary and imaging secondary mirrors were exceptions to this rule since they incorporated a number of custom designed parts to meet stability requirements and/or increase the number of degrees of freedom (DOF) needed for alignment. The secondary mirror mounts employ Newport model 562, 3-axis manual linear stages and series 562F manually controlled tip/tilt mounts. The Newport stages provide five DOFs, with the sixth (roll about the optic axis) being a feature of the custom designed interface plates used to mount the secondary mirrors.

The FIT optic axis is positioned 11.5" above the plane of the optical bench. This height was driven to a large extent by the center height of the large 11.5" collimating primary mirror (OAP). From a stability perspective, it is obviously desirable to keep the optics as close as possible to the table. We made an effort to compensate for the relatively high optic axis height by increasing the stability and stiffness of the mounting hardware deployed throughout the testbed.

The entire optical bench is surrounded by a light tight enclosure that provides stray light control and possibly minimizes turbulence within the beam path. The frame was constructed using extruded aluminum beams, which support the plastic sheets and films used for stray light control. The enclosure while not perfect, does bring the background level down to the 5.6KC bias level (dark frame) of the Finger Lakes CCD camera.
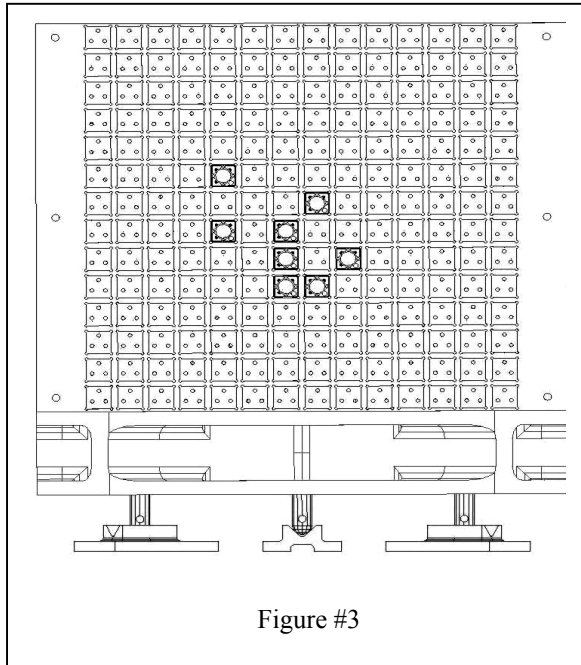
2.2.1 Primary Mirror Array (PMA)

Figure #3

The primary mirror array consists of a precision machined aluminum plate incorporating a 14" x 14" rectilinear grid of mounting surfaces (on 1" centers) as shown in Fig. #3. The plate is supported using a three-point mount that allows for coarse adjustments in azimuth, elevation and height. Each 12.5mm diameter spherical mirror element is bonded to a custom interface plate and then coupled to a Melles Griot model 17ASM003 piezoelectric tip-tilt mount. The seven mirror "stacks" are arranged in a minimally redundant Golay [2,3] pattern that may be manually reconfigured to evaluate the performance of a variety of segment configurations.

Seven Thorlabs model MDT693 three-channel controllers are used to drive the mirror segments in tip, tilt and piston. These controllers are slaved through a National Instruments (NI) PXI-1000B chassis containing two PXI-6704 analog output cards. The PXI-6704 cards deliver computer initiated commands to each of the seven Thorlab controllers, which then parse out commands to the 21 PZT actuators on the PMA. The NI cards have been programmed to preserve the state of the last commanded position for each of the 21 actuators. This feature allows the operator to exit the control program (Labview) without compromising the alignment of the PMA and provides a level of protection in the event of a system reboot or unexpected power failure. The piezoelectric mounts have a total travel range of +/- 3.5um. Due to safety concerns, each Thorlabs controller has been modified (in hardware) to limit actuator displacement to approximately +/- 2.5um.

2.3 System Software

Data acquisition and control is handled by a 2Gh Pentium based computer operating under Windows 2000. The interface to the "executive" software is a Graphical User Interface (GUI) constructed using National Instruments Labview software. Data collected using the executive computer is saved to disk and backed up daily using an external drive. The executive software is responsible for the following actions:

- Scene selection
- Motion control (cameras, filter wheel)
- Lamp radiance control
- Data acquisition (CCD cameras)
- Selecting and implementing desired phase retrieval / phase diversity algorithms
- Phase plate actuator control
- Data Storage

3. Source Module (SM)

The source module was designed to introduce a range of pinholes, filters, and scenes to the testbed, providing an array of options for testing phase retrieval and diversity algorithms and for studying various alignment configurations. The SM (fig #5) employs a computer controlled, 250W Oriel Quartz Halogen lamp used to illuminate a complement of filters, scenes and point sources. The lamp housing was ordered with an optional 4-element aspheric condenser lens (f/0.7) and a plano-convex secondary (f/1.3) so that its output could be efficiently coupled into a liquid waveguide (LWG) "fiber" (3mm core diameter) manufactured by Oriel. At this time, the Oriel lamp housing is located on the surface of the FIT

optical bench. In the near future, we will relocate this lamp off of the table in order to improving stray light, vibration and thermal performance (stability).

Light exiting the SM is essentially Lambertian over the over the acceptance angle of the optical system. Without the use of supplementary focusing optics, light exiting the waveguide is uniform enough to illuminate extended scenes, and intense enough to back illuminate a non-resolved point source (~15um pinhole), providing sufficient flux at the detector. The SM uses a computer controlled, six-position filter wheel for wavelength/bandwidth selection and a computer controlled linear stage for scene insertion. The filter wheel is currently populated with the filter set shown in fig #4,

Center	FWHM
632.8 nm	40nm
632.8 nm	11 nm
700 nm	55 nm
700 nm	40 nm
700 nm	12.3 nm

Figure #4

though provisions have been made to augment this selection by repopulating or replacing the existing wheel. The filter wheel is positioned between the liquid waveguide and the plane of the scene plate. In order to maximize throughput, the separation between the LWG and the plane of the rotating filter wheel was minimized, as was the overall light source to scene distance. The liquid waveguide is desirable from a stray light, vibration and output uniformity standpoint. However, its large divergence angle (~62 degrees) makes it difficult to couple into the FIT optical system. By limiting this separation to ~ 0.75", flux at the focal plane was high enough to allow operation in an exposure regime commensurate with system stability requirements. When running with our smallest aperture (15um pinhole) and a broadband source we manage to get ~80,000c/s at the focal plane. This is enough flux to allow us to operate at 80% of full well even when using one of the narrow bandpass filters. When working with narrow filters, the exposure times need to be increased from tenths of a second to tens of seconds. Even with these relatively long exposure times, initial phase retrieval work was not crippled by image blur resulting from systematic jitter.
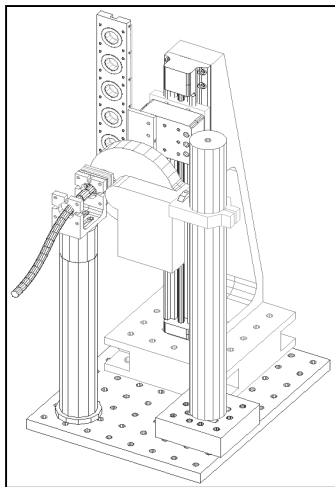

Figure #5

The SM accepts scene plates that kinematically mate with the computer controlled vertical stage (fig. #5). Each scene plate holds six scenes that may be commanded into precise alignment at the focal plane of the collimating optics. All scenes incorporate fiducials that are used to assist in the angular alignment of the image with respect to pixels in the CCD focal plane. Scene clocking angles are toleranced so that the edge of an image runs along a single row of pixels at the focal plane (~3 arc-sec). Individual scenes are mounted to "carriers" prior to their insertion into a scene plate. The interface between the carrier and scene plate is tightly toleranced to aid in the co-registration of scenes within the scene plate. The X-Y decenter (repeatability) for each scene will set to be better than 5um in both axes. Given a system magnification of 1.5X, the X-Y repeatability for a given scene is on the order of one 9um X 9um pixel at the focal plane.

A bypass fold mounted on a kinematic base may be installed in front of the scene plate to facilitate the use of alternate sources such as lasers and interferometers. This feature was incorporated to aid future alignment work, and to serve as an independent method for verifying end-to-end system performance.

4.0 FIT Optical Alignment Overview

The initial goal of the alignment plan was to assign a coarse alignment to the PMA plate prior to its insertion into the testbed. This was driven primarily by the approach used to perform the coarse alignment, which required moving the PMA through a series of independent metrology steps that sequentially refined the alignment. The alignment sequence utilized both mechanical and optical metrology to set piston, tip and tilt for each of the seven mirror segments; resulting in nominally phased mirror at the sub-micron level.

The initial coarse alignment consisted of two stages of mechanical alignment followed by an optical refinement in the form of Dispersed Fringe Sensing (DFS). The application of these three techniques resulted in a nominally phased array plate with piston variations on the order of 1micron. At this point, from the perspective of "top-level" system integration, the PMA was treated as a 5" diameter spherical mirror. Fine phasing was performed after the array plate was

incorporated into final FIT optical configuration (Fig. #1). The details of these operations will be present in subsequent sections of this paper.

4.1 Mechanical Assembly/Alignment of PMA

The initial step in the mechanical alignment was to set each of the manually controlled actuators (Melles Griot tip/tilt mounts) to the mid-point of travel and then integrate the mounts with the PMA. The distribution of segments on the array plate was consistent with the non-redundant pattern described earlier and represents the "baseline configuration" for future alignment steps. With the PMA positioned on a granite table, a precision dial indicator was used to set the vertex of each segment to a fixed height above the "reference flat" which is positioned near the center of the distribution. All of these adjustments were made using the manual controls provided on the Melles Griot mounts. At this time, we also took a first cut at setting the segment tip/tilt orientations using these same controls, with positional feedback provided by the dial indicator. At the completion of this step, the vertex of each mirror segment lay in a plane with vertex-to-vertex variations on the order of +/-10um.
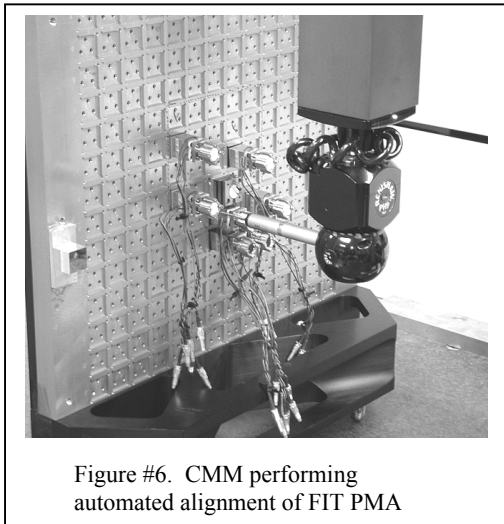
4.1.2 Refined Mechanical Alignment of PMA

Figure #6. CMM performing automated alignment of FIT PMA

The sequence of steps described in section 4.1 yields an array of spherical mirrors; however the vertex of all seven segments lies in a fixed plane above the array plate. The ultimate goal is to align and phase all seven segments so that the vertex of each mirror segment is precisely positioned on a spherical surface having a 4000mm radius of curvature. A Brown and Sharpe DEA Gamma 1204 Coordinate Measuring Machine (CMM) controlled by PC DEMIS was employed to complete this phase of the alignment. A parametric model constructed using PC DEMIS allowed the CMM to precisely measure the coordinates of the vertices for all seven mirrors to within +/-12um. The software then compares the measured results with modeled data and presents the computed differences to the operator. In an iterative sequence, the segments were measured, adjusted and then re-measured until the measured and modeled values converged. At the completion of his process, the PMA was aligned in piston to within +/- 12um. There was a significant delay (10 days) between completing the CMM work and integrating the array plate into the FIT optical system. As such, the quoted piston errors resulting from the CMM alignment process are probably worst case values. Based on historical work, we believe the CMM should be capable of meeting this requirement to at least ±5um.

4.2 Coarse Phasing of FIT PMA at Radius of Curvature

After completing CMM based mechanical alignment, the PMA was set up at its radius of curvature as shown in Fig. 7. This setup is not a permanent part of the FIT testbed, but rather an intermediate setup used to coarse phase the PMA plate prior to incorporating the PMA into the final FIT configuration. The 15um pinhole was placed on axis with the PMA plate using a theodolite. A white light source (or laser) was coupled into a 15um pinhole that was positioned on axis at the radius of curvature of the primary mirror array plate (4000 mm). Light reflected from the mirror segments (PMA) impinges on a beamsplitting cube and is then delivered to both a CCD camera and a microscope. A reticle placed at the focal plane of the CCD camera (with 10X objective) was used as a fiducial, assisting in the co-alignment of all seven returns (mirror segments) at focus. Based on the angular separation of the returns (at focus), the CMM alignment was good to better than +/-10um. If we assume comparable errors in axial piston, the mechanical alignments reduced the piston errors (between segments) from millimeters to tens of microns. In order to further improve coarse phasing we employed an optical technique known as dispersed fringe sensing. The DFS was able to reduce piston variations from

tens of microns to the sub-micron level. Once the PMA was removed from the ROC setup and installed in the FIT optical system, white light interferometry was used to phase the segments to within tens of nanometers. Since FIT is currently operating in an open loop mode, such precision is likely to be short lived as the system evolves in response to environmental conditions within the lab.

Figure #7
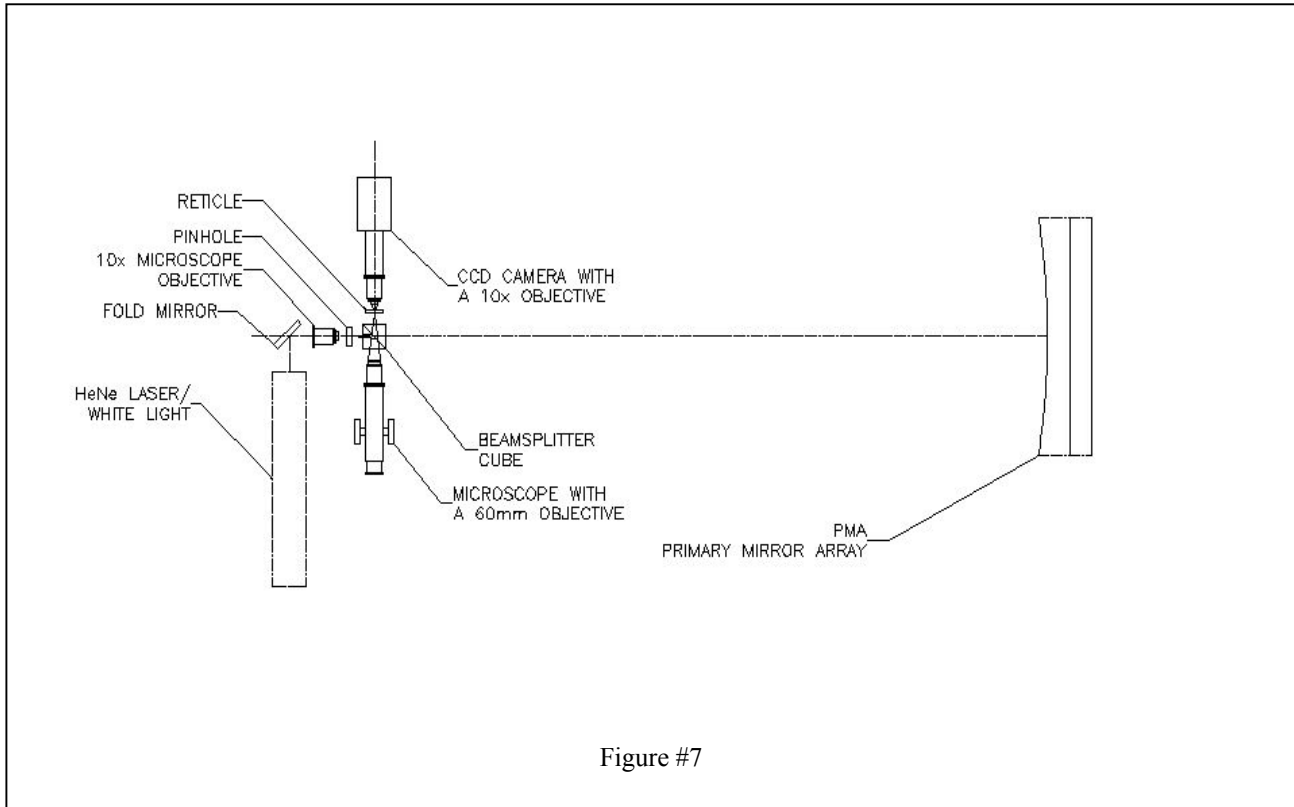
4.2.1 Coarse Phasing PMA With Dispersed Fringe Sensor (DFS)

Coarse phasing of the PMA was performed using a Dispersed Fringe Sensor (DFS) and then later refined with White Light Interferometry (WLI). Both of these techniques were employed in a qualitative manner, with visual feedback via a CRT monitor being the arbiter of success. The fringes used to coarse phase the PMA were generated with a 300-lp/mm transmissive diffraction grating that was inserted into the converging beam between the beamsplitting cube and the CCD camera (Fig. 7). The DFS disperses light from two co-aligned (but de-phased) segments and then delivers this light to a video camera for inspection. When using a polychromatic source, light is dispersed spectrally across the CCD focal plane so that each column of pixels corresponds to a single wavelength. The residual piston error from the CMM alignment manifests itself as a phase difference between the two overlapped images at the focal plane. This phase difference results in an intensity modulation along the dispersion direction that is the sum of the field intensities from the two de-phased segments. The period of the fringes is a measure of the absolute phase difference between the two segments under study, while the angular tilt of the fringes provides information on the "sense" of the correction needed null the two segments. The dynamic range of the DFS is large, with fringe visibility dependent on focal plane sampling (Nyquist) and the dispersion of the grating (or other dispersive element). The nominal optical path difference (OPD) resulting from the CMM based alignment (~ +/-10um) was well within the several hundred micron capture range of the FIT DFS.
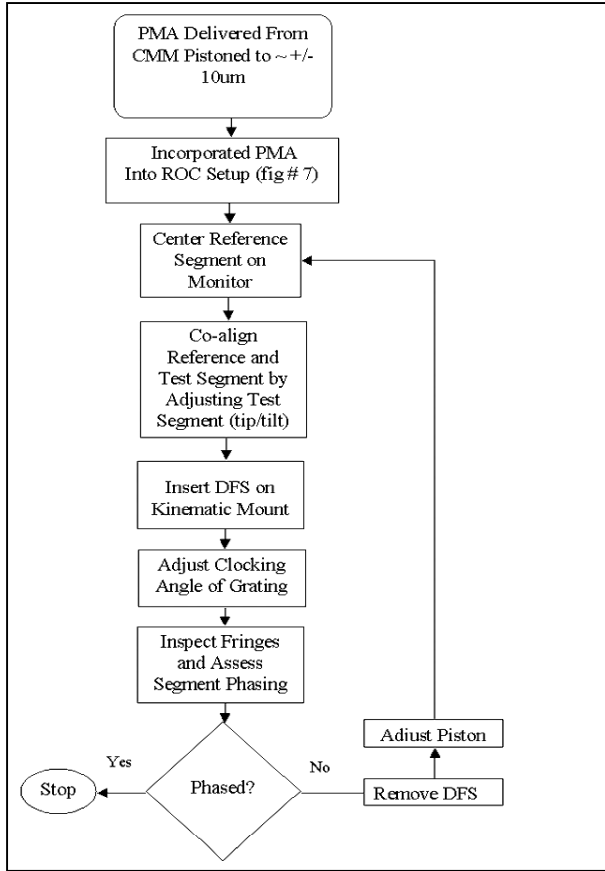
Figure #8

The DFS simplified the task of phasing the segments since it provided real time feedback on the piston offset between the reference and "test" segments. Alternatively, we could have systematically "hunted" for white light fringes without using the DFS, though this option was not overly appealing for obvious reasons. Each "segment pair" exercised in the alignment of the PMA consisted of the reference segment (Seg. #4) and a test segment. The reference segment (located near the center of the distribution) served as a datum surface for phasing the remaining six mirrors.

Figure #9 shows the sequence of steps involved in phasing a two mirror segments. This routine is repeated pairwise, until all of six segments have been phased with the reference segment. All piston adjustments and subsequent co-alignments (tip/tilt) were performed with the grating removed from the setup. Piston corrections were introduced by sequentially rotating the three set-screws located on the test segment mount while maintaining sight of the return on a monitor. The manual actuation on the PZT mounts is extremely sensitive, making it difficult to piston and realign the images at ROC. In the future, we may add an automated translator having a few hundred microns of travel so that more controlled amounts of piston may be introduced. This improvement could potentially minimize the need for frequent grating removal, thus minimizing the possibility of walking a return off of the focal plane during the phasing process. The orientation of the grating is also critical when phasing segments with the DFS. Maximum fringe contrast occurs when the dispersion direction is perpendicular the baseline between segment pairs [7]. In order to maintain this condition, the grating was mounted on a manually controlled rotary stage that was adjusted independently for each 2-segment combination.

Figure #9 shows three typical images from the DFS. The first and third images show interference fringes resulting from a +/-12um piston difference between the reference and test mirrors. The center image shows the nominal "nulled" condition indicating that the mirror segments were close to being optimally phased.
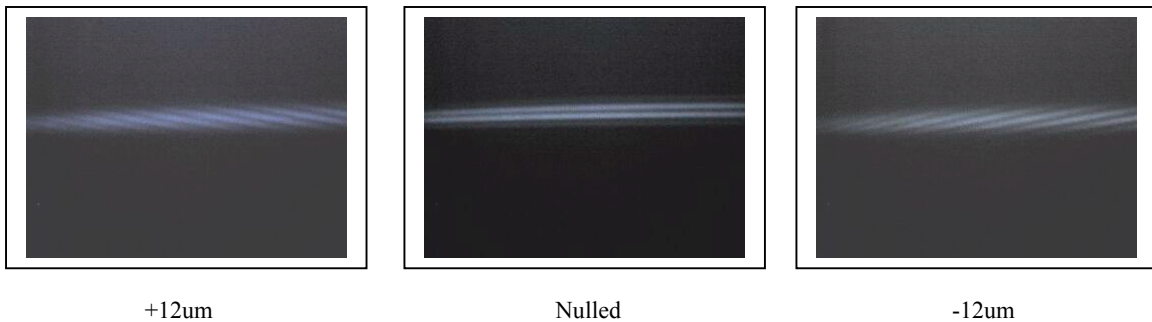

+12um   Nulled   -12um

Figure #9. Interference fringes resulting from two de-phased FIT mirror segments. One segment was treated as a reference while the second was scanned axially in piston during the nulling process. Note the change in fringe inclination on either side of null.

4.3 Alignment and Integration of FIT Optics

After completing the coarse phasing as described in section 4.0, the seven segments making up the PMA were all phased to within ~1 micron. From an integration standpoint, the PMA was now treated as a spherical mirror, with the central reference segment (flat mirror) being at the vertex of the sparse aperture array. The central segment was scribed with a cross that defined the vertex of the primary mirror array.

The assembly/alignment of the FIT testbed utilized the chief ray pointing direction originally established for the ROC work. The theodolite used to position the pinhole on axis with the PMA was already setup normal (AZ and EL) to the PMA and centered on the vertex of the flat mirror segment. An alignment cube was added to the optical bench that preserved the pointing directions for both the X and Y axes. The cube was placed just below the mirror segment #3, so that it is out of the clear aperture of the system.

Once the PMA was aligned normal to and centered on the chief ray, a theodolite was used to pin the X-Y centration of the plate. A second theodolite was used to guide in a 4-degree azimuthal tilt with respect to the optic axis. Next, the large collimating OAP was installed and aligned to the system aided by alignment fiducials and a plane mirror bonded to the rear surface of the optic. The collimating and imaging optics were then introduced and aligned in azimuth and elevation with respect to the centrally mounted alignment cube.

After aligning the secondary mirrors, we installed the Pellicle beamsplitter and the two CCD cameras at the aft end of the system. The camera accepting the transmitted beam was mounted on a motorized translation stage that was aligned to track the exit ray of the system. The second camera intercepting the reflected beam from the Pellicle is set at a fixed position. The camera on the motorized stage may translated in axial focus for phase retrieval measurements, but typically remains at a "fixed" defocused position during the simultaneous image capture required for phase diversity.
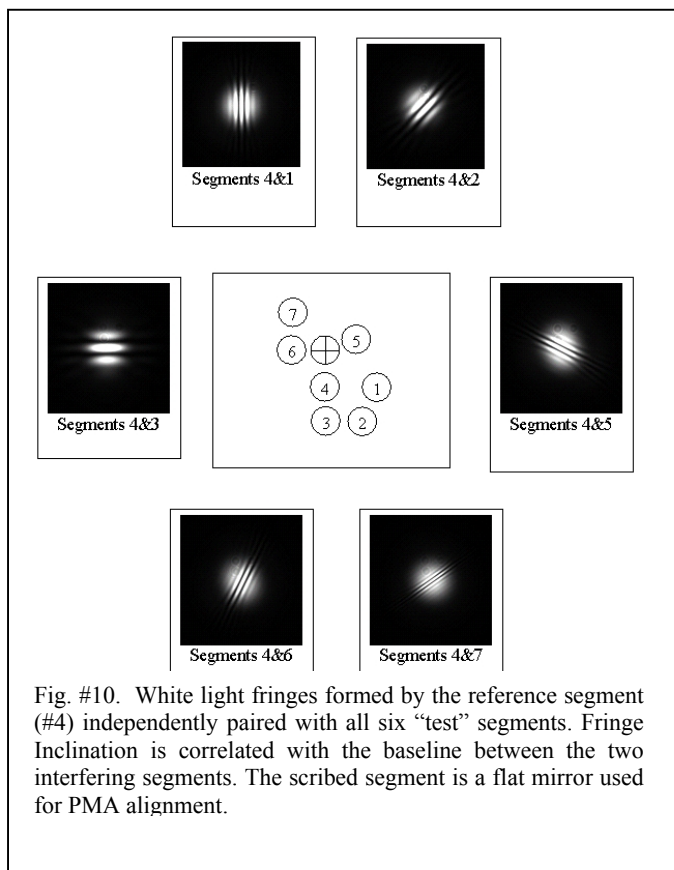

Fig. #10. White light fringes formed by the reference segment (#4) independently paired with all six "test" segments. Fringe Inclination is correlated with the baseline between the two interfering segments. The scribed segment is a flat mirror used for PMA alignment.

It should be noted that the axial despace for all components was set with a precision good to only a few millimeters. We plan to use a portable CMM to refine these settings to something on the order of +/-15um when it becomes available. The angular alignments were set to within five arc-seconds of the prescription, however the uncertainty in these values is estimated (in some cases) to be significantly higher (~ 30arc-seconds).

Much of this uncertainty results from the mount design used for the collimating and imaging secondary mirrors. Once the optic was placed in the mount, there was no direct access to the rear surface of the optic. The uncertainty in angle is primarily driven by our estimate of the maximum possible wedge between the rear surface of the optic and the backplane of the mount.

With the exception of the central reference flat, none of the FIT optics have fiducials marking the center of the optic. For this initial phase of the alignment, we estimated the X and Y decenters to within a few hundred microns of their prescribed values. At a later date, we plan to refine the overall system alignment using both phase retrieval techniques and a CMM.

From an aberration standpoint, the most sensitive components in the system are the collimating and imaging aspheres. According to the Zemax model, these components are relatively insensitive to angular (tip/tilt)

alignment errors on the order of our alignment uncertainties. A 30-arcsecond tilt in AZ or EL (on either secondary) does not significantly degrade the nominal on axis performance (0.04 λ RMS @ 632.6nm) of the "ideal system". Going 1.2 mm off axis, the figure is still on the order of a hundredths of a wave.

The centration of the collimating secondary mirror is the most sensitive alignment with respect to the aspheres. A 1mm Y-decenter results in a ~0.12 λ RMS (on axis) figure error. This is a significant portion of the measured 0.25λ RMS already quoted. Future experimentation will allow us to deconvolve these errors and potentially separate out systematic alignment errors from errors introduced at the PMA plate. Taking this into account, the initial results were quite good considering the time delay between segment phasing and the commencement of phase retrieval (section #5).

4.4 White Light Interferometry

With the PMA nominally phased and integrated into the FIT optical system (fig. #1) we proceed to refine the coarse phasing using White Light Interferometry (WLI). The source was an unresolved 15um pinhole placed at the focal plane of the collimator optics. The pinhole was backlit with broadband source consisting of a 7mm diameter liquid waveguide illuminated using the Quartz Halogen lamp described in section 3.0.   Images were collected using one of the FIT science cameras positioned at the system focus. Fringe acquisition was performed pairwise, with each measurement using the reference segment (#4) paired with one of the remaining six mirror segments. The formation of white light fringes strictly implies that the optical path difference between the two interfering segments is effectively zero (within the coherence length of the incident radiation). This process was repeated for all six pairings as shown in figure #10. Small corrections in piston on the order of ~30nm were applied after initial white light fringe capture to improve the contrast and symmetry of the image. In most cases, the white light fringes were acquired relatively easily using computer-controlled PZT actuators.

 This alignment was not intended to be rigorous. Our goal was to follow a reasonably fast and direct path leading to coarse phasing of all seven segments. In the near future, the FIT testbed will incorporate software that can sense and control segment-to-segment piston errors using both DFS and WLI methodologies.

For a segment pair having a baseline separation of one-inch, the white light fringes are visible over a range of approximately 800nm from the "nulled" position. The actual capture range using this technique is roughly double this number ±800nm (with 1" baseline separation) if we take into account piston motions on either side of null. As the baseline separation between segments increases, the fringe count increases and the fringe visibility decreases [8]. We estimate that segment-to-segment piston variations on the order of ≤ 60nm are routinely sensed and controlled using "visual sensing" and corrections imparted at the keyboard.
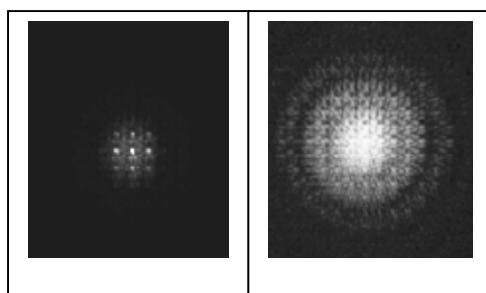
5.0 Initial System Performance

Figure #11. Linear and log-stretched FIT PSF with all seven segments. 632.8nm, 40nm wide bandpass filter.

Figure #11 shows "first light" results from the FIT testbed. The images show the superposition of all seven segments at focus, taken at 632.8nm (40nm wide) using a 15um pinhole. The first image is shown on a linear scale while the second is log stretched.   Initial phase retrieval results show an RMS wavefront error of ~λ/4 ± λ/28 over all seven apertures. The maximum and minimum wavefront errors measured on a single aperture were ~λ/10 ± λ/31 and ~λ/20 ± λ/32 respectively [5]. These numbers represent "first light" results that incorporate a number of error sources that are easily controlled.   The largest single factor compromising system wavefront performance is likely temporal drift within in the PMA.   There was a gap of approximately 24 hours between the coarse phasing operation and the time when the phase retrieval data was collected. As a result, the analysis carries with it thermally induced alignment errors introduced over the ensuing 24 hours. Additional sources of error include (but are not limited to) uncertainties in subaperture location and an uncharacterized spectral transmittance function for the 632.8nm bandpass filter. Future data sets will incorporate these refinements.

6.0 System Stability and Environmental Factors

The laboratory environment plays a critical role in the performance of FIT. Since FIT is essentially an interferometer, its performance is highly dependent on temperature and vibration stability within the laboratory environment. Though stability was a significant driver, the system was also engineered to be cost efficient. In keeping with this theme, most of the optical mounts were off the shelf components, with custom hardware being reserved for critical components such as the PMA plate. While operating in an open loop mode, it is desirable to have sub-micron level stability over the duration of an experiment (up to several hours). As we transition to closed-loop operation, drifting will be corrected as long as the control bandwidth is above the nominal drift-rate and the magnitude of the corrections fall within the dynamic range of the actuators. This requirement is generally satisfied for all observed thermally induced drifts.

6.1 Temperature Induced Line of Sight and Differential Drift

Temperature control within the laboratory is held to better than ±0.7º C over a typical 24 hour period. As the temperature varies over this range, the testbed exhibits a temperature-induced drift in both the X and Y centroids. Generally, these motions are expressed as image walk at the system focal plane, and tend not to significantly de-phase the PMA plate. This Line of Sight (LOS) motion is common to all seven segments and likely results from a global change in the elevation of the PMA (or other optical component(s)) in response to temperature variations. Over a 24 hour period, these LOS drifts may be as large as ~100 pixels which is on the order of the diffraction limited spot size of the system (~ 1.2mm).

In addition to global (or common) LOS motions, we also experience differential, or segment–to-segment drifts that can potentially de-center and de-phase the mirror elements. Figure #12 shows such behavior as indicated by two FIT mirror segments (4 and 7) over a 65 hour time interval. For this particular set of data, there is a divergence in the Y centroids between the two segments (which at maximum is about 20 pixels) over the first 30 hours. These motions represent "typical behavior" that has been observed for all seven-mirror elements. The maximum change in temperature over this 65 hour period was ~ ± 0.5 ºC with a 1ºC decrease over the first 30 hours.

The thermal effects impacting testbed stability are a function of the overall laboratory environment and localized heat loads introduced by the 250-Watt QTH source. This situation will be improved (to some extent) when we convert to a longer liquid waveguide allowing the lamp housing to be located outside of the FIT enclosure.

The mirror mounts on the PMA exhibit hysterisis. The cumulative effects of even repeatable "thermal variation" tend to (over time) walk the segments out of the control range of the PZTs. In order to keep the system in a state of readiness, we implement periodic "maintenance adjustments" using a combination of coarse (manual) and fine (PZT) controls to keep the 7-segments nominally phased at or near the mid range of travel for the PZT actuators. Even under extreme conditions, it is anticipated that the system will remain stable enough complete a days worth of data acquisition.

For a typical segment pair having a 1" baseline separation, fringe visibility (as viewed on a CRT monitor) is detectable over a range of ~ ±800nm. This is a reasonably large range, encompassing approximately 1/4 of the total travel range of the PZTs. Differential piston errors greater than ~800nm (from null), would present challenges since these images are not likely to show fringing. Recovery from large piston errors may be achieved using the DFS technique as described in section 4.2.1. The use of the diffraction grating (DFS), allows the CCD camera to sense piston errors up to several hundred microns.

Long-term stability requiring only minor corrections in tip/tilt and piston (applied using PZTs) have been maintained for periods up to several weeks. On other occasions, large thermal variations (several degrees C) have grossly de-phased the array plate over a three-day period. Under such circumstances, the induced piston errors are well beyond the dynamic range of the PZT actuators (±2.5um), requiring manual intervention using the coarse actuators to re-phase the system.

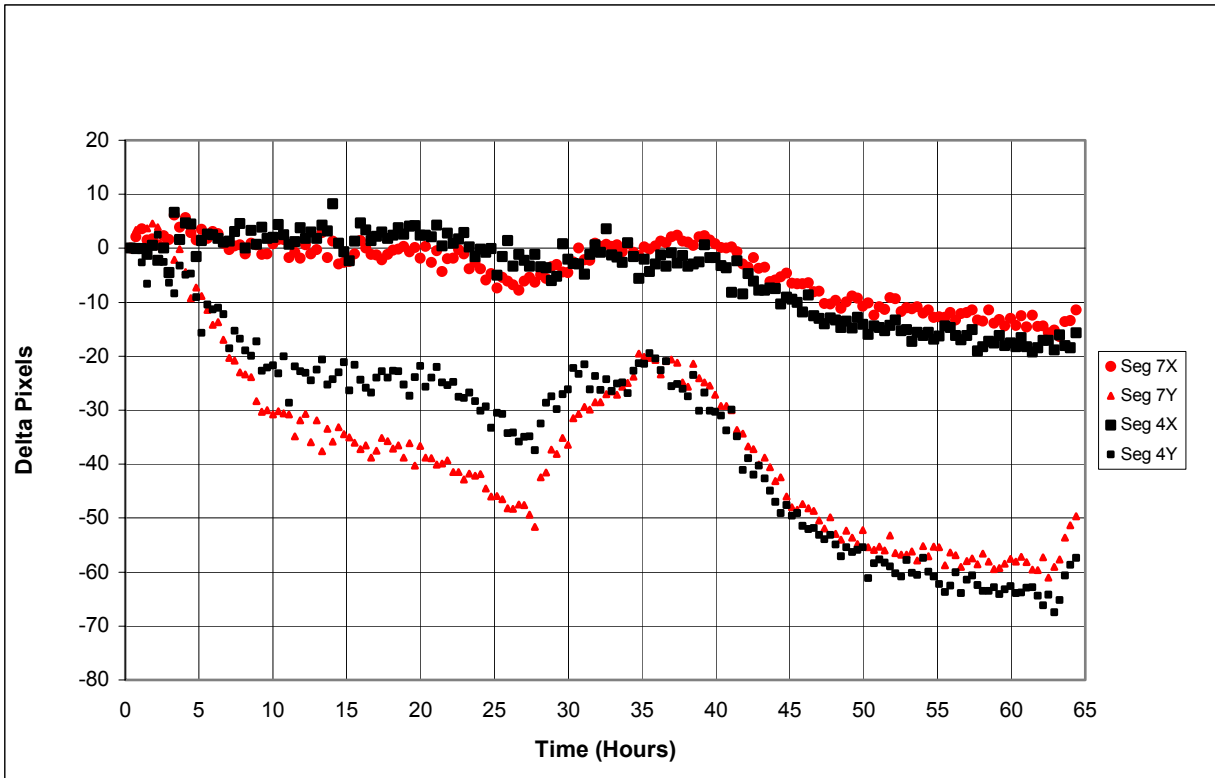**Temporal Stability of FIT Testbed**

Figure #12

7.0 Summary and Conclusions

The Fizeau Interferometer Testbed has been assembled and aligned in its Phase I configuration (7-segments). A LabView-based GUI was developed that provides fine control over tip/tilt and piston (for each segment) in addition to controlling the CCD camera and its linear stage. Using this interface, we collected some initial performance data while operating in an open-loop mode. The measured wavefront resulting from this early work was ~ λ/4 RMS (measured using phase retrieval). The time delay between segment phasing and data acquisition was in excess of 24 hours, so the resulting data carries with it errors caused by temporal drifting.

The thermal stability of the system appears to be sufficient for performing most if not all of the intended open-loop experiments. The stability issues will obviously improve when we run in a closed-loop mode as long as the disturbances are slow-acting and within the dynamic range of the PZT actuators. Initial stability data indicates that the system should operate within the control range of the PZT actuators for reasonably long periods of time (weeks). Methods exist for rephrasing the segments should they drift out of the control range of the PZTs.

The recently completed source module has been aligned to the system which providing efficient access to a range of pinholes and spectral filters. Extended scene and calibration masks have been fabricated, and will soon be mounted and aligned to the appropriate scene plate(s). We are now in a position to begin a complete calibration of the FIT optical system and ultimately leading to the closed loop control of the testbed.

Work is currently under way to expand the functionality of the Labview interface, providing it with the capability to call the complete complement of phase retrieval/diversity algorithms cited for use on the testbed. After the system calibration has been completed, FIT will be exercised in both open and closed loop operating modes using both point sources and extended scenes.   All phase 1 activities will be performed with 7-segments arranged in a Golay configuration. In the future, the mirror count may be increased up to 30 elements in order to study the impact of various U-V plane samplings on system performance and to demonstrate that the control algorithms and methodologies developed for the phase I system will work in the much more complex 30-element system (phase II) needed for actual space missions.

ACKNOWLEDGEMENTS

References

1. Carpenter, K., Schrijver, C. J., Allen, R. J., Brown, A., Chenette, D., Danchi, W., Karovska, M., Kilston, S., Leitner, J. A., Liu, A., Lyon, R. G., Marzouk, J., Mazzuca, L. M., Moe, R. V., Walter, F., "The Stellar Imager (SI): A Revolutionary Large-Baseline Imaging Interferometer at the Sun-Earth L2 Point", in *New Frontiers in Stellar Interferometery,* SPIE proceedings, Vol 5491, 2004

2. Golay, M.J.E. 1971, "Point Arrays Having Compact, Nonredundant Autocorrelations,'" J. Opt. Soc. Am., 61, 272-273

3. S.W. Golumb, "Point Arrays Having Compact, Non-redundant Autocorrelations", IEEE 61, 272-273, 1971.

4. Lyon, R.G., Carpenter, K.G., Huet, H., Cottle, P., Petrone, P., Dogoda, P., Liiva, P., Marzouk, J., Solyar, G., Mazzuca, L., Zhang, X. 2004, ``Building the Fizeau Interferometer Testbed", Proc. IEEE Aerospace Conf. 2004

5. Lyon, R.G., Carpenter, K.G., Petrone, P., Dogoda, P., Liiva, P., Marzouk, J., Solyar, G., Mazzuca, L., "Fizeau Interferometry Testbed Wavefront Control", in *Optical, Infrared, and Millimeter Space Telescopes,* SPIE proceedings, Vol 5487, 2004

6. Mazzuca, L., Carpenter, K.G., Lyon, R.G., Petrone, P., Huet, H., Cottle, P., Dogoda, P., Liiva, P., Marzouk, J., Solyar, G., Mozurkewich, D., Amstrong, J. T., Zhang, X., Mundy, L., "The Fizeau Interferometer Testbed(FIT): Developing and Testing the Technologies Needed for Space-Based Interferometric Imaging Systems", in *New Frontiers in Stellar Interferometery,* SPIE proceedings, Vol 5491, 2004

7. F. Shi, A. Lowman, et al, "Segmented mirror coarse phasing with a dispersed fringe sensor: experiments on NGST's wavefront control testbed," Proc. SPIE 4850-51, Waikoloa, Hawaii, 2002.

8. F. Shi, C. Ohara, et al, "Segmented mirror coarse phasing with white light interferometry: modeling and experimenting on NGST's wavefront control testbed," Proc. SPIE 4850-59, Waikoloa, Hawaii, 2002.

9. Zhang, X., Carpenter, K.G., Lyon, R.G., Huet, H., Marzouk, J., Solyar, G., ``The Fizeau Interferometer Testbed", Proc. IEEE Aerospace Conf. 2003